Turbulent Von Karman Swirling Flows

Sébastien Poncet, Roland Schiestel, Romain Monchaux

Turbulent Von Kármán Swirling Flows

S. Poncet[1], R. Schiestel[2], and R. Monchaux[3]

[1] MSNM-GP, UMR 6181, Technopôle Château-Gombert, 38 rue F. Joliot-Curie, 13541 Marseille - France poncet@l3m.univ-mrs.fr
[2] IRPHE, UMR 6594, Technopôle Château-Gombert, 49 rue F. Joliot-Curie, 13384 Marseille - France schiestel@irphe.univ-mrs.fr
[3] Service de Physique de l'Etat Condensé / GIT, CEA Saclay, 91191 Gif sur Yvette - France romain.monchaux@cea.fr

We investigate the turbulent Von Kármán flow generated by two counter-rotating flat or bladed disks. Numerical predictions based on a Reynolds Stress Model (RSM) are compared to velocity measurements performed at CEA [2]. This flow is of practical importance in many industrial devices such as in gas-turbine aeroengines. From an academic point of view, this configuration is often used for studying fundamental aspects of developed turbulence and especially of magneto-hydrodynamic turbulence.

1 Geometrical model and numerical approach

The Von Kármán geometry is composed of two counter-rotating disks ($R = 92.5$ mm) enclosed by a stationary cylinder ($R_c = 100$ mm) (Fig.1). The interdisk spacing H can vary in the range $10 - 180$ mm. We use bladed disks (n blades of height h) to ensure inertial stirring or flat disks for viscous stirring. The rotation rates Ω_1, Ω_2 can be increased up to 900 rpm. The main flow is controlled by three parameters: the ratio between the two rotation rates $\Gamma = -\Omega_2/\Omega_1$, the aspect ratio of the cavity $G = H/R_c$ and the Reynolds number $Re = \Omega_1 R_c^2/\nu$. In the following, $G = 1.8$ and $\Gamma = -1$.

Our numerical approach is based on one-point statistical modeling using a low Reynolds number second-order full stress transport closure (Reynolds Stress Model, RSM) sensitized to rotation effects and already validated for $\Gamma = 0$ and a wide range of G and Re [1]. To model straight blade effects, we add a volumic drag force in the equation of V_θ the tangential velocity component: $f = n\rho C_D(\Omega_{1,2}r - V_\theta)|\Omega_{1,2}r - V_\theta|/(4\pi r)$, where ρ is the fluid density, $C_D = 0.5$ the drag coefficient and r the local radius. The procedure is based on a finite volume method using staggered grids for mean velocity components with axisymmetry hypothesis. A 120^2 (resp. 160^2) mesh in the (r, z) frame is used in the smooth (resp. bladed) disk case. About 20000 iterations (several

hours on the bi-Opteron 18 nodes cluster of IRPHE) are necessary to obtain the numerical convergence of the calculation.

2 Results

The mean flow is decomposed into two poloidal cells (fig.1) in the (r,z) plane. In the viscous stirring case, the flow structure is of Batchelor type close to the periphery of the cavity at $r/R_c = 0.81$ (fig.2a) and so exhibits five distinct zones: two thin boundary layers on each disk, a shear layer at mid-plane and two cores on either side of this layer. For an inertially driven flow, the mean flow is divided into three main regions (fig.2b): a very intense shear layer at mid-plane and two fluid regions close to each bladed disks. At the top of the blades, there is a strong decrease of $|V_\theta|$ interpreted as the wake of the blades. The turbulence is mainly confined in the equatorial plane (fig.3a,1) and is found to be almost isotropic in that region for viscous stirring. When one imposes inertial stirring, the normal components are increased by a factor 10 (fig.2b) and a much higher shear stress is obtained around $z^* = 0$. The weak discrepancies between the two approaches are attributed to the appearance of strong coherent structures observed in the experiments [2].

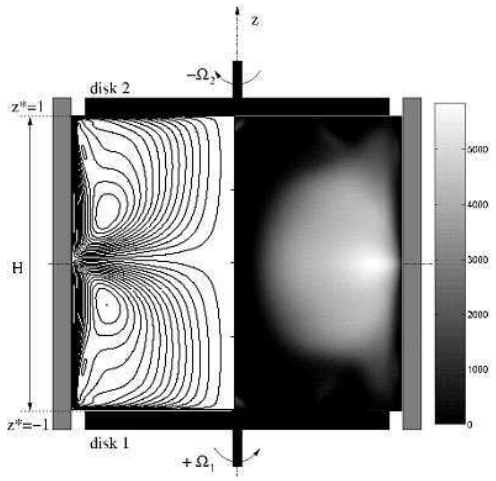

Fig. 1. Sketch of the cavity in the smooth disk case. Computed (left) streamlines and (right) iso-turbulence Reynolds number $Re_t = k^2/(\nu\epsilon)$ for $Re = 6.28 \times 10^5$.

3 Conclusion

We proposed an easy and efficient way to model the effects of impellers on the turbulent Von Kármán flow. A parametric study according to the flow

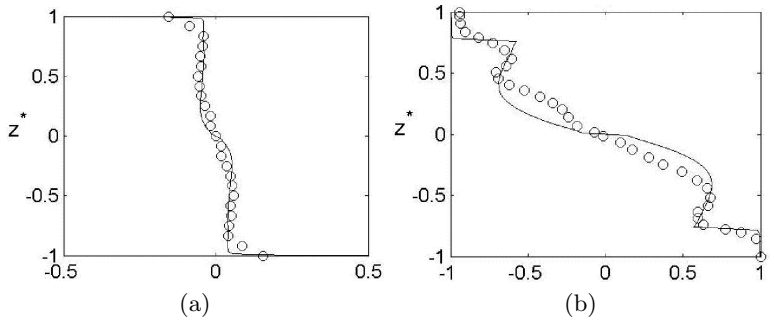

Fig. 2. Axial profiles of $V_\theta/(\Omega_1 r)$: (a) viscous stirring ($Re = 6.28 \times 10^5$, $r/R_c = 0.81$), (b) inertial stirring ($Re = 2 \times 10^5$, $n = 8$, $h/R_c = 0.2$, $r/R_c = 0.4$). (lines) RSM, (∘) LDV data of [2].

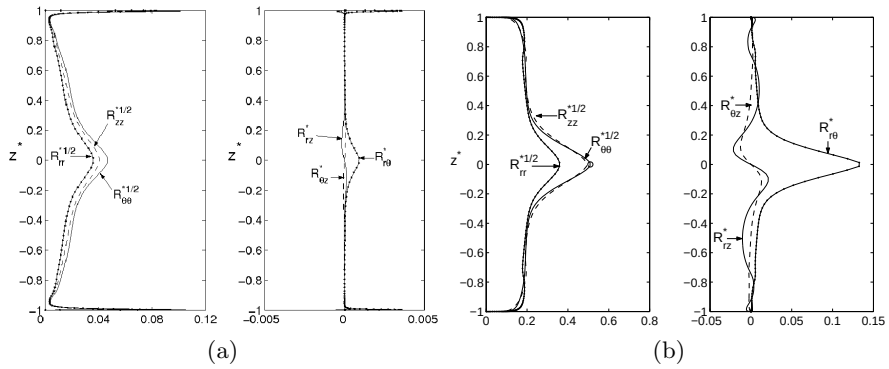

Fig. 3. Axial profiles of the Reynolds stress tensor at $r/R_c = 0.81$: (a) viscous stirring ($Re = 6.28 \times 10^5$), (b) inertial stirring ($Re = 2 \times 10^5$, $n = 8$, $h/R_c = 0.2$) (RSM). (∘) LDV data of Ravelet [2] for $R_{\theta\theta}^{*1/2}$.

control parameters has been performed for viscous and inertial stirrings. In particular, we highlighted three main transitions: Batchelor / Stewartson, Batchelor / torsional Couette, one-cell / two-cell regimes. Some calculations for curved blades are still in progress.

References

1. S. Poncet, M.P. Chauve, R. Schiestel: Phys. Fluids **17(7)**, 075110 (2005)
2. F. Ravelet: Bifurcations globales hydrodynamiques et magntohydrodynamiques dans un écoulement de Von Kármán turbulent. PhD Thesis, École Polytechnique, Palaiseau (2005)